

Supporting Information: 3D multiscale
characterization of the human placenta: bridging
anatomy and histology by X-ray phase-contrast
tomography

Jakob Reichmann, Anne Schnurpfeil, Sylvia Mittelstädt, Patrick Møller
Jensen, Vedrana Andersen Dahl, Anders Bjorholm Dahl, Carina Weide, Eva
von Campenhausen, Hector Dejea, Paul Tafforeau, Christopher Werlein,
Danny D. Jonigk, Maximilian Ackermann, Klaus Engel, Julia Gallwas,
Alexander Dietz, Mir Fuad Hasanov, and Tim Salditt^{*}

^{*}Corresponding Author: Tim Salditt, tsalditt@gwdg.de

sample	size	emb. mat.	setup	vox. size [μm]	E [keV]	man. fig.
H1	full organ	70% EtOH	BM18	19.19	92	2a, 4, 5cd
	3-5 mm biopsy (x3)	FFPE	GINIX	0.65	13.8- 15	9
	3 mm full biopsy	70% EtOH	GINIX	0.65	13.8	
	full organ	70% EtOH	μCT	50	150	6a
	3mm biopsy (x3)	FFPE	μCT	16	60	
	UC	70% EtOH	μCT	15	100	5a
	infarctious region	70% EtOH	GINIX	0.65	13.8	8b
H2	full organ	70% EtOH	BM18	19.19	92	
	UC	70% EtOH	BM18	3.033	68.5	2b, 8c
	full organ	70% EtOH	μCT	50	150	
	full organ zoom	70% EtOH	μCT	20	150	
H3	2 biopsies	70% EtOH	GINIX	0.65	15	7ab, 8d
H4	full organ	70% EtOH	BM18	19.19	92	
	full organ	70% EtOH	μCT	50	150	
PE	full organ	70% EtOH	BM18	19.19	92	
	UC	70% EtOH	BM18	3.033	68.5	
	full organ	70% EtOH	μCT	50	140	
	3mm full biopsy	70% EtOH	GINIX	0.65	13.8	8a
CoV	full organ	70% EtOH	BM18	19.19	92	
	3 cm pieces (x 4)	70% EtOH	BM18	3.033	68.5	3
	UC	70% EtOH	BM18	3.033	68.5	
	full organ	70% EtOH	μCT	20	150	
	3 cm piece	70% EtOH	μCT	14	80	
CoV (biopsy)	8 mm biopsy	FFPE	GINIX	0.65	15	

Table S1: Overview of placentas studied: 4 healthy (H), 1 preeclampsia (PE), and 1/2 COVID-19 (CoV) placentas. The table shows sample sizes, preparation methods, scanning setups, voxel size, and X-ray energy / tube voltage.

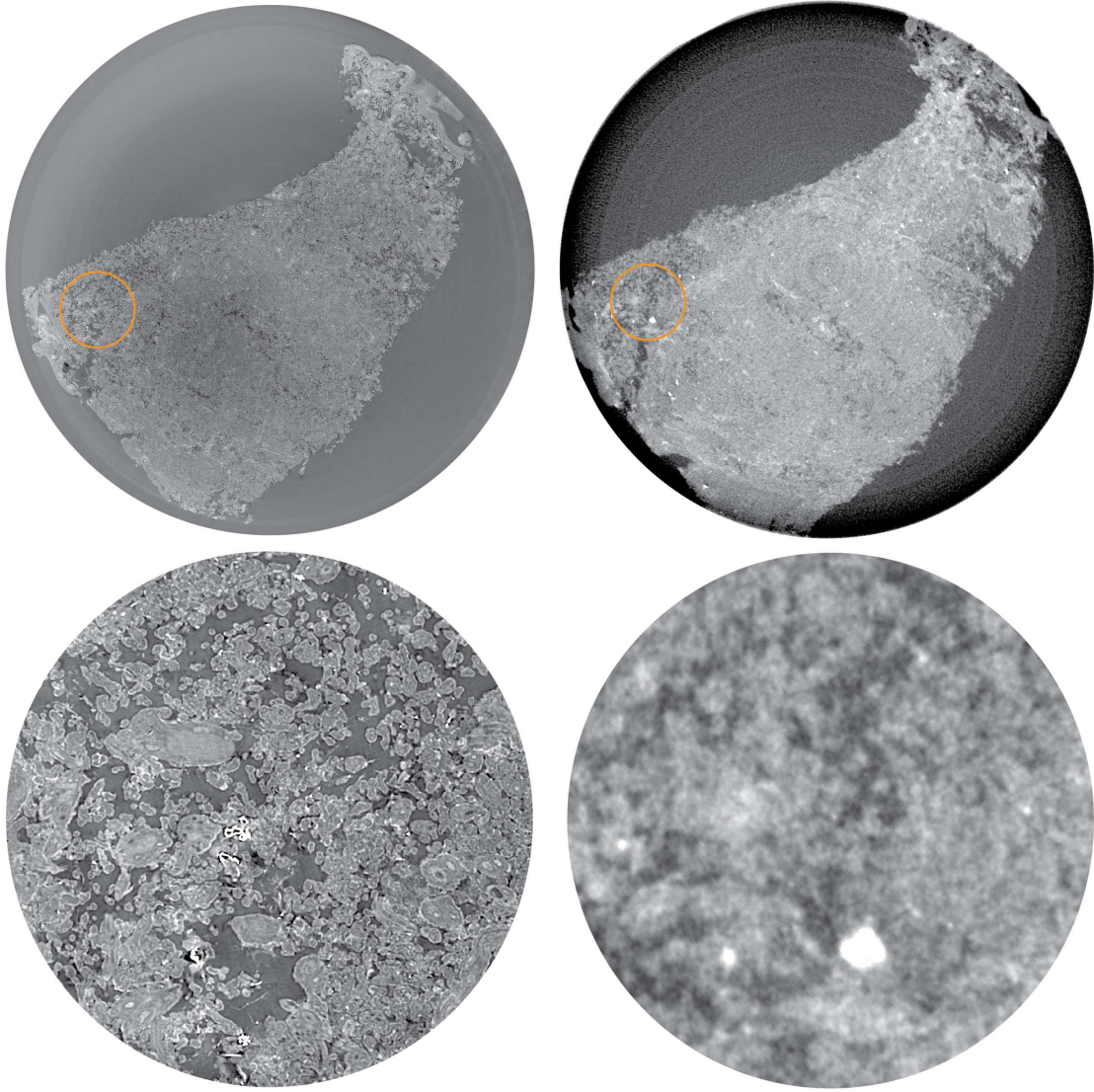


Fig. S1: Qualitative image quality comparison between synchrotron scan (BM18-HR), left, and in-house scan right (μ CT-setup). Same sample as shown in Fig. 2 in the main manuscript.

Movie S1 The supplementary video presents an animation of the rendered dataset of a healthy human placenta (Cinematic Anatomy, Siemens Healthineers, Germany). It starts with the removal of the surrounding shredded agarose through histogram manipulation. The placenta is then rotated and virtually cut in the xy-plane, thereby revealing the 3D cytoarchitecture of the organ. Finally, thresholding allows for the visualisation of parts of the vascular tree.



Fig. S2: Cinematic rendering of the fetal side of a healthy human placenta.

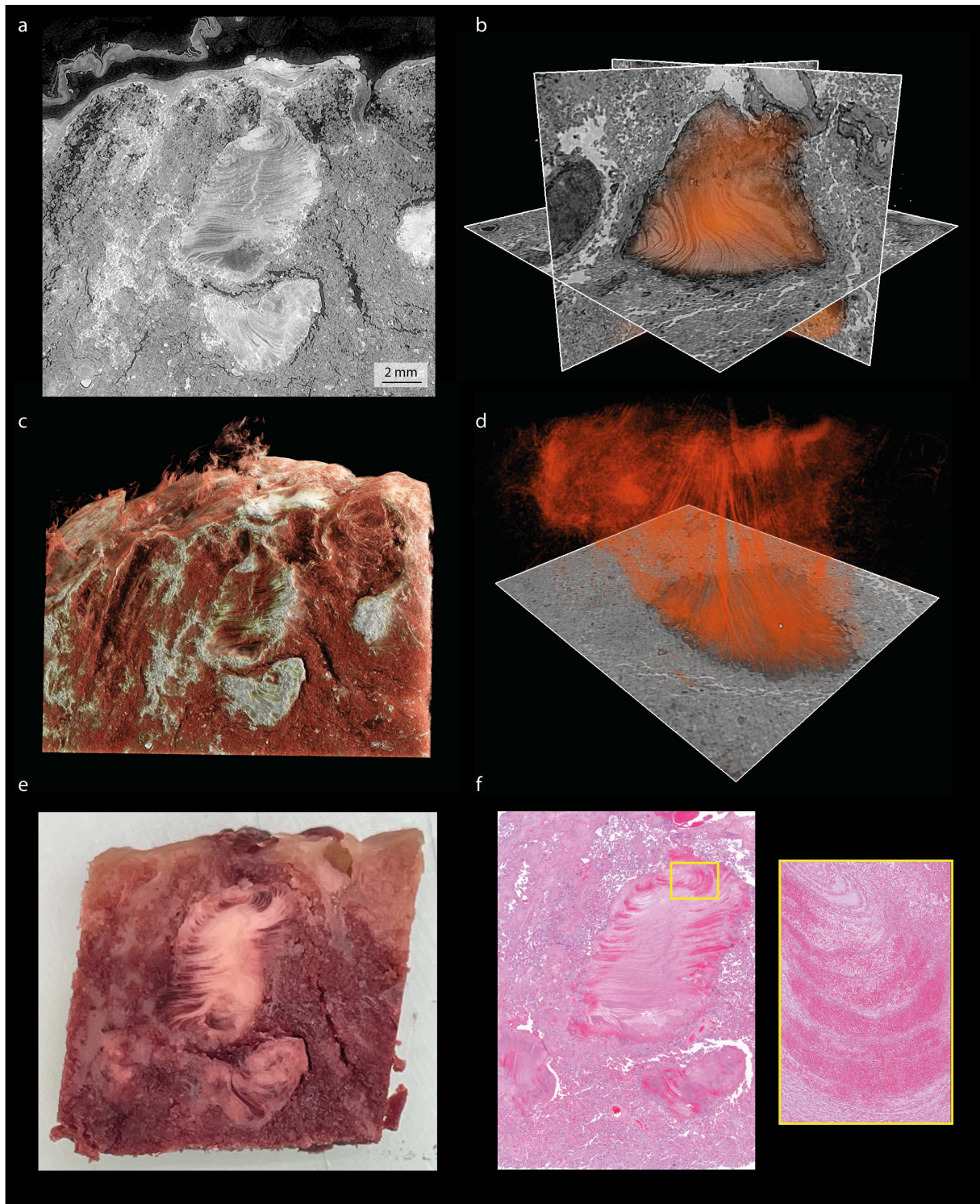


Fig. S3: Intervillous subacute thrombosis including laminar-structured lesions. **a** Region of interest in scan of intact human placenta (BM18-T) with clearly distinguishable intervillous thrombus with laminar structured lesions (lines of Zahn). **b** Three orthogonal slices with the segmented intervillous thrombus in the center (orange). **c** Depiction of same thrombotic region, rendering using CA. **d** Slice through the intervillous thrombus with rendered laminar-structured lesions. **e** Photograph of cut out tissue piece with intervillous subacute thrombosis before histological analysis. **f** Histological of same tissue region (top tissue layer, visible on the photograph in (f)) with zoom at laminar-structured lesions (yellow box).

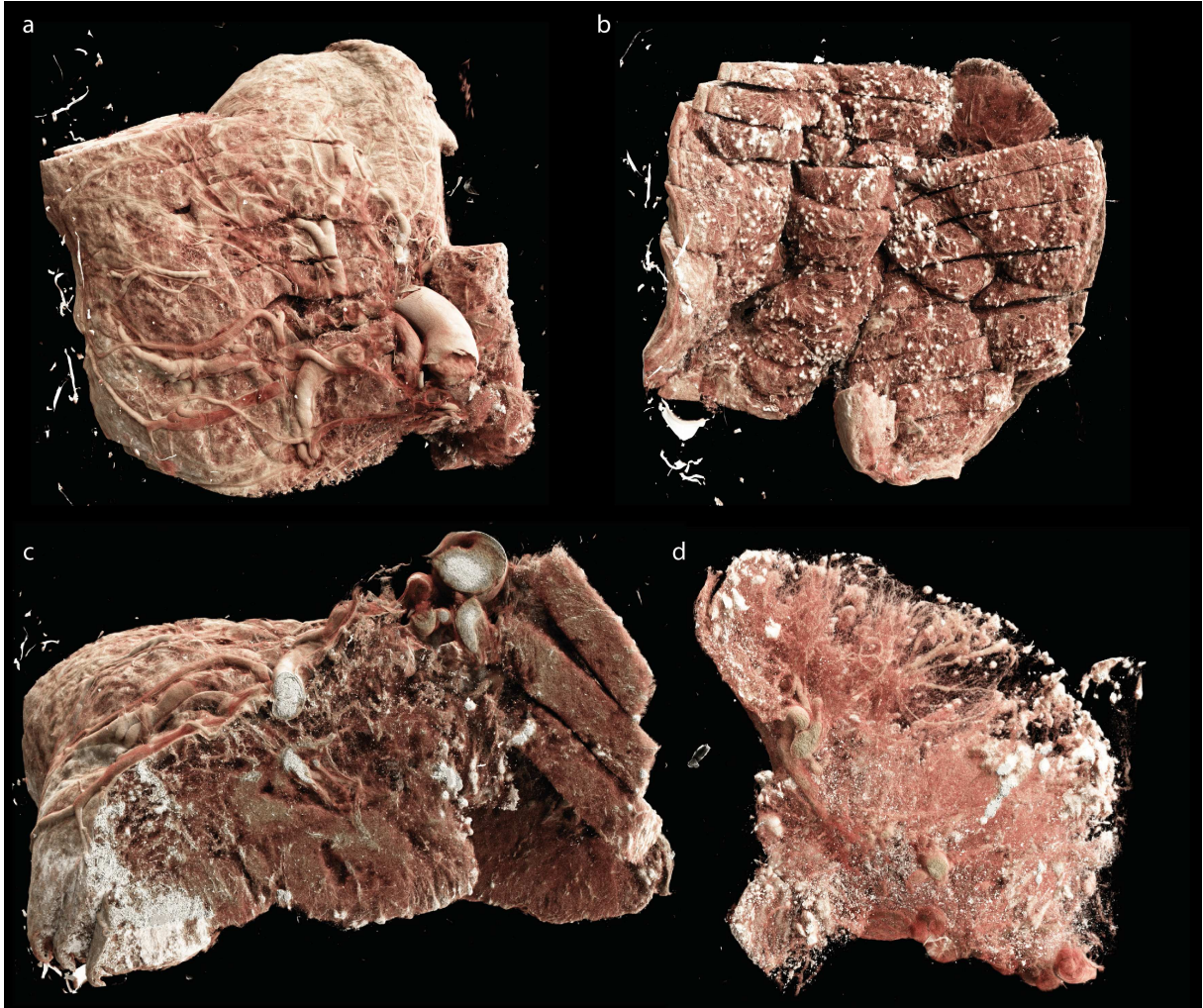


Fig. S4: Cinematic rendering (Cinematic Anatomy) of SARS-CoV-2 infected placenta. The placenta was routinely sectioned for preceding visual tissue inspection. The chorionic plate with the vascular tree emerging from the umbilical cord is visible in **a**, while **b** shows a view on the basal plate. In **c**, a virtual cut through the placenta gives a view on the placental tissue morphology and organization with an additional rendering where outer placental regions were made transparent in **d**. Notably, the basal plate in **b** shows an accumulation of highly absorbing features which might indicate placental calcification.



Fig. S5: Photographs of sample intact placentas and sample preparation. The **top row** shows fresh placenta samples immediately after extraction. In the **center row**, the degassing process (left) is depicted, as well as after the completed preparation (center) and on the sample on the sample stage at the BM18 beamline (right). At the **bottom**, the placenta is depicted after removing it from the sample box and after sectioning and sample extraction for histological analysis.

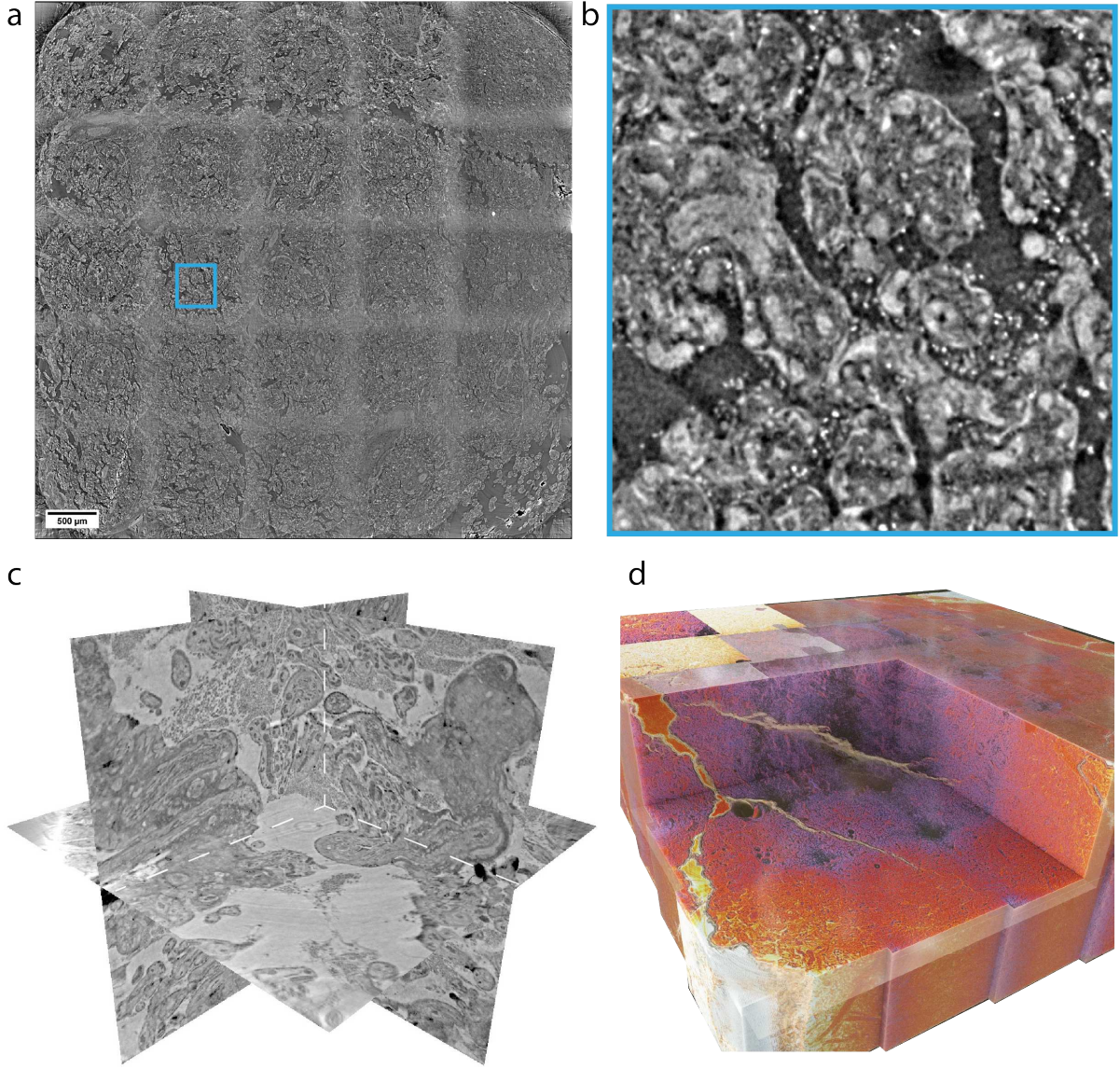


Fig. S6: Datasets of FFPE human placental tissue acquired at the P10-PB setup. **a** Slice from $5 \times 5 \times 3$ (x,y,z) stitched volume ($2 \times 2 \times 2$ binned) of SARS-CoV-2 infected paraffin-embedded placental tissue with zoom-in (**b**) to showcase image quality (full resolution). The tissue biopsy has a diameter of ≈ 5 mm. **c** Three orthogonal slices from an liquid-embedded (70% EtOH) tissue sample (same as Fig. 7a in main article). **d** Cinematic rendering of a paraffin-embedded biopsy punch recorded with the P10-PB setup.

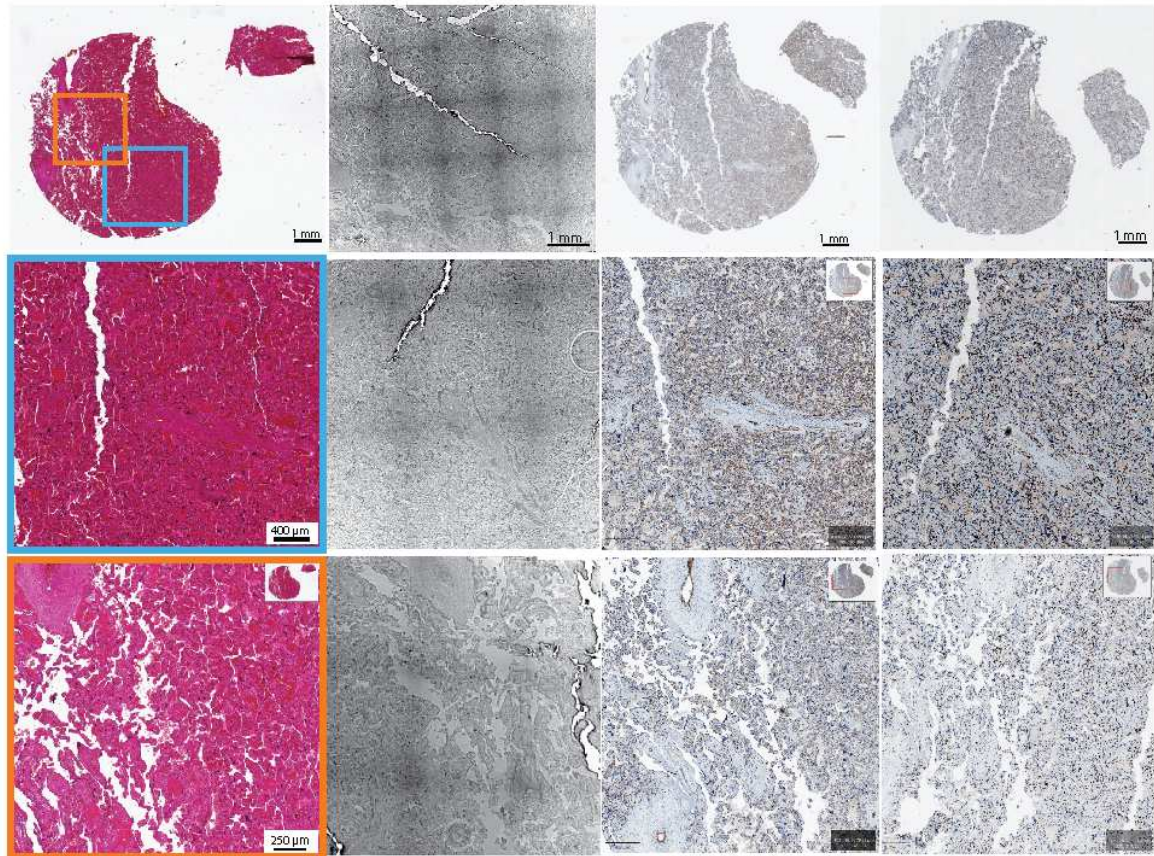


Fig. S7: Correlative imaging of conventional histology (H&E, first column), stitched XPCT volume (second column), CD31 immunohistochemistry (third column) and CD163 immunohistochemistry (fourth column) in ascending magnification (row 1-3). Correlation from XPCT volume data to conventional histology and subsequent immunohistochemical analyses is possible. Especially on higher magnification, placental blood vessel (upper left corner) and placental villi are readily identified on XPCT. Note the increased presence of CD163 positive Hofbauer cells in the placental villi (fourth column).

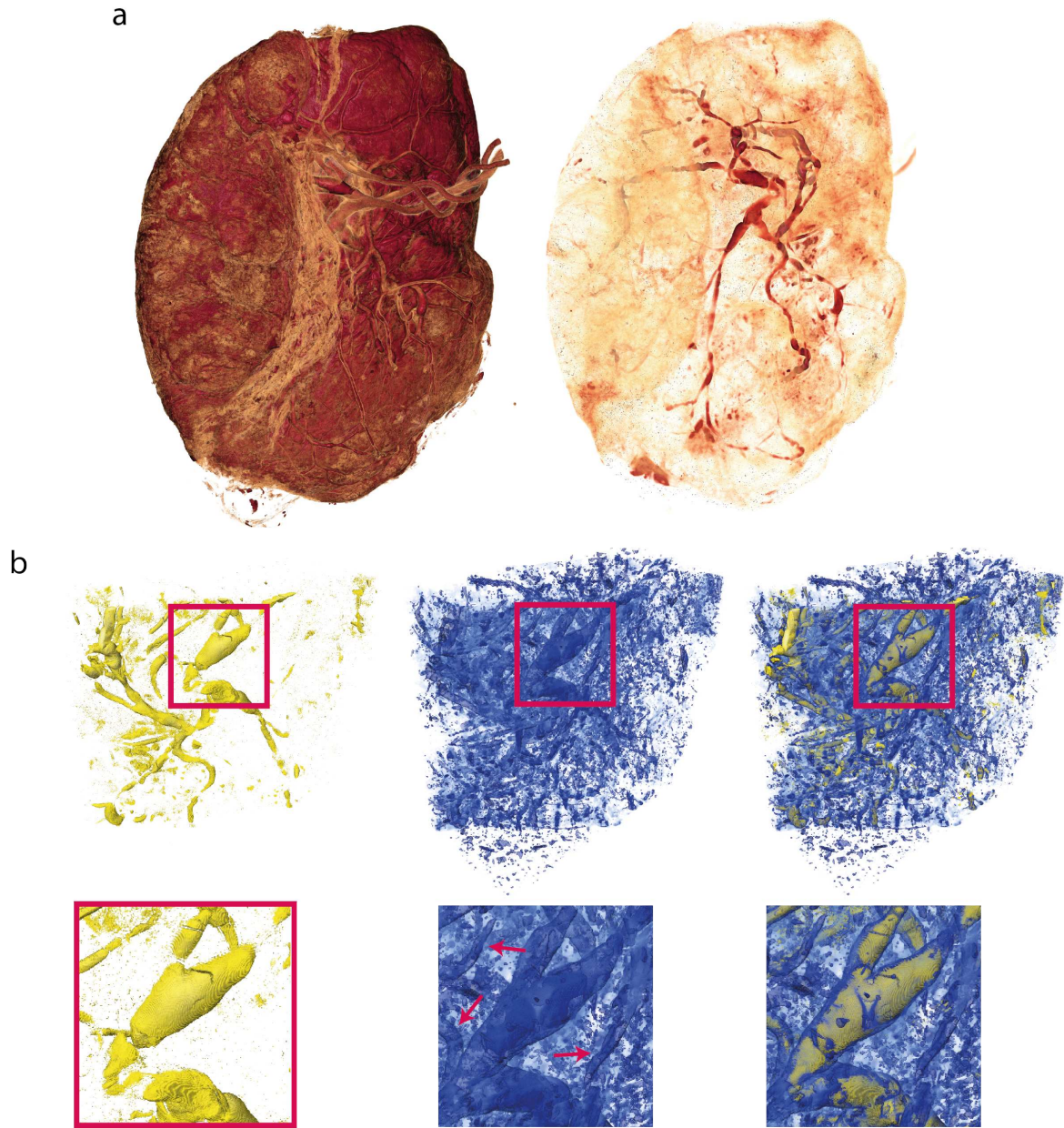


Fig. S8: **a** 3D rendering of entire human placenta (Cinematic Anatomy, Siemens Healthineers, Germany) using an edge enhancement gradient shader (left). By setting a suitable threshold value and changing the opacity parameter for each gray value, high-contrast features such as calcified blood can be made visible (right). Both renderings were created with NVIDIA IndeX (NVIDIA IndeX, Santa Clara, USA). **b** Rendering of vascular tree (yellow), segmented vascular tree using the prediction by a trained U-Net with sparsely-annotated data (blue) and overlay.

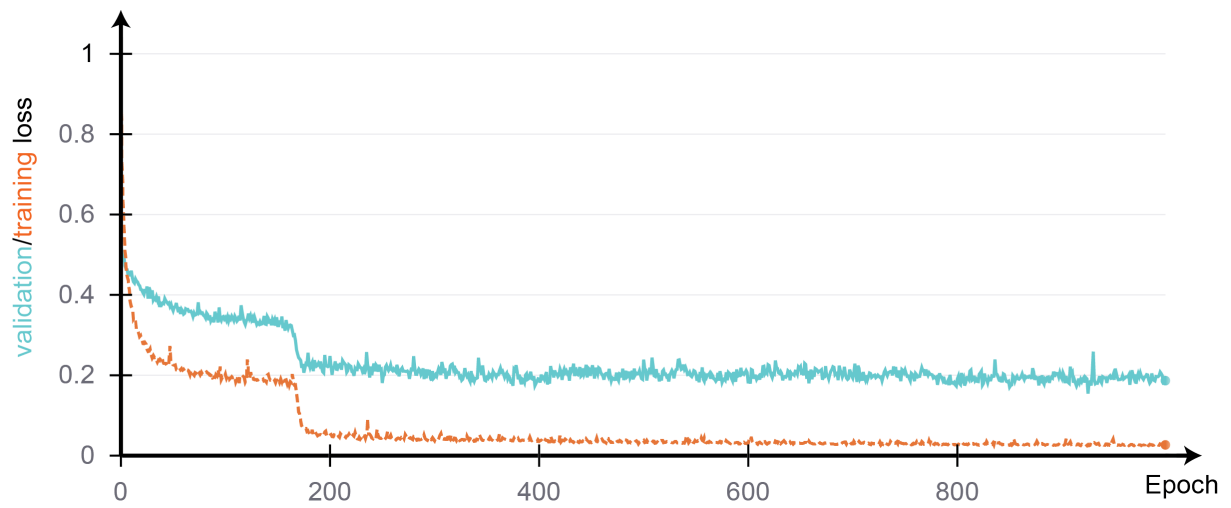


Fig. S9: Training (orange) and validation (turquoise) loss for training of V-net with manually, sparsely annotated vascular network of healthy placenta (see main manuscript for detailed procedure).